

The periodic standing-wave approximation: computations in full general relativity

Napoleón Hernández

*Department of Physics, University of Utah, Salt Lake City, UT 84112,
and Department of Physics & Astronomy and Center for Gravitational Wave Astronomy,
University of Texas at Brownsville, Brownsville, TX 78520**

Richard H. Price

*Department of Physics & Astronomy and Center for Gravitational Wave Astronomy,
University of Texas at Brownsville, Brownsville, TX 78520*

Abstract

The periodic standing wave method studies circular orbits of compact objects coupled to helically symmetric standing wave gravitational fields. From this solution an approximation is extracted for the strong field, slowly inspiralling motion of binary black holes and binary neutron stars. Previous work on this project has developed a method using a few multipoles of specially adapted coordinates well suited both to the radiation and the source regions. This method had previously been applied to linear and nonlinear scalar field models, to linearized gravity, and to a post-Minkowski approximation. Here we present the culmination of this approach: the application of the method in full general relativity. The fundamental equations had previously been developed and the challenge presented by this step is primarily a computational one which was approached with an innovative technique. The numerical results of these computations are compared with the corresponding results from linearized and post-Minkowski computations.

I. BACKGROUND AND INTRODUCTION

Due to successes in numerical relativity, there is now a good understanding of many features of the gravitational waves from the inspiral and merger of comparable mass black holes[1, 2, 3, 4, 5, 6, 7, 8, 9, 10, 11, 12, 13, 14, 15, 16, 17, 18] There are, however, areas that are still best investigated with an approximation method for the slow inspiral epoch. One area is the evolution and gravitational waveform during the slow inspiral (but strong field) epoch, since there are too many orbits for numerical relativity to be feasible. Another area is the case of mass ratios too large for numerical relativity, but not large enough for particle perturbation methods. A slow inspiral approximation method is also useful as a starting point for a better understanding of the radiation reaction fields acting on an inspiralling hole.

The Periodic Standing Wave (PSW) project is meant to provide such an approximation. This method seeks a numerical solution for a pair of sources (black holes, neutron stars) in nondecaying circular orbits with gravitational fields that are rigidly rotating, that is, fields that are helically symmetric. Because the universality of gravitation will not permit outgoing waves and nondecaying orbits, the solution to be computed is that for standing waves. An approximation for slowly decaying orbits with outgoing radiation is then extracted from that numerical solution.

This work has progressed through several stages. In the first stage[19, 20, 21, 22, 23], a nonlinear scalar fields model was investigated, and numerical methods were developed to deal with the special mathematical features that would be common to all standing-wave, helically symmetric computations. These features include: (i) a mixed boundary value problem (regions of the domain in which the equations are hyperbolic and other regions in which they are elliptic); (ii) an iterative construction of nonlinear standing wave solutions; (iii) the extraction from the standing wave solution of an approximate outgoing wave solution. Reference [23] introduced a new technique that promised to reduce the computational burden: “adapted coordinates” that were well suited to the geometry of the problem both near the sources and far from them. In Ref. [23] it was shown that with these coordinates good results could be computed by keeping only a very small number of multipoles, typically just the monopole and quadrupole moments. That method was applied to linearized

*current address: JP Morgan, 277 Park Avenue, Floor 12, New York, NY 10172-0003.

general relativity in Ref. [24] and to the post-Minkowski approximation to general relativity in Ref. [25]. In the current paper we apply this method, PSW in adapted coordinates, to full general relativity.

The mathematical infrastructure for this is rather involved. It includes the definition of standing waves for nonlinear fields; extraction of the outgoing solution; the adapted spatial coordinates; the multipole decomposition in adapted coordinates; the reduction to helical symmetry for tensorial fields; the full vacuum field equations; the inner boundary conditions on surfaces outside black holes. This infrastructure has been thoroughly documented in earlier papers, and the complete infrastructure is presented in Ref. [25]. Rather than give yet another lengthy presentation of this infrastructure, here we will give only enough of the mathematical background necessary in order to explain the numerical results we are presenting, and to compare them with other numerical results.

The rest of the paper is organized as follows. Sec. II develops the mathematical description of helically symmetric tensor fields in terms of “helical scalars,” quantities that are functions only of corotating coordinates. The field equations of general relativity, and of its weak field approximations are given for these helical scalars, along with boundary conditions on these fields. Section III discusses two important aspects of the numerical approach to our computations: (i) “discrete spherical harmonics” on our computational grid, and (ii) the use of the *Maple*TM symbolic manipulation language to handle the complexity of the equations to be solved numerically. The numerical results produced by these methods are presented in Sec. IV, and are discussed in Sec. V.

II. THE MATHEMATICAL PROBLEM

A. The field equations and coordinates

We start with the concept of a strong field source region and a weak field source region. The strong field source region is close to the inner computational boundary, surfaces with spherical topology around the black holes, and close to them but far enough from the horizon for computations to be feasible. We invoke a set of coordinates labelled t, x, y, z for which the spacetime metric $g_{\mu\nu}$ deviates only slightly from the flat metric $\eta_{\mu\nu}$ at large coordinate distances from the binary sources.

We impose helical symmetry by requiring that in these coordinates there be a Killing vector given by

$$\xi = \partial_t + \Omega (x\partial_y - y\partial_x) \quad (1)$$

where Ω is a constant. It is convenient to define a rotating coordinate system by

$$\tilde{t} = t \quad \tilde{z} = z \quad \tilde{x} \equiv x \cos \Omega t + y \sin \Omega t \quad \tilde{y} \equiv -x \sin \Omega t + y \cos \Omega t. \quad (2)$$

and to introduce two cylindrical coordinates systems: r, z, ϕ in terms of x, y, z by the usual flat space formulas, and $\tilde{r}, \tilde{z}, \tilde{\phi}$ in terms of $\tilde{x}, \tilde{y}, \tilde{z}$ also by the usual flat space formulas. We note that Eq. (1) is equivalent to

$$\xi = \partial_t + \Omega (\tilde{x}\partial_{\tilde{y}} - \tilde{y}\partial_{\tilde{x}}) = \partial_t + \Omega \partial_{\varphi} = \partial_{\tilde{t}}, \quad (3)$$

We follow the formulation of Landau and Lifschitz [26, 27] for the Einstein equations, which encodes the geometric information in the densitized metric

$$\mathfrak{g}^{\alpha\beta} \equiv \sqrt{|\det g|} g^{\alpha\beta}. \quad (4)$$

To simplify the field equations, we choose to have our coordinates obey the harmonic condition

$$\mathfrak{g}^{\alpha\beta}_{,\beta} = 0, \quad (5)$$

we define the inverse $\mathfrak{g}_{\alpha\beta}$ of our basic field $\mathfrak{g}^{\alpha\beta}$ by

$$\mathfrak{g}^{\alpha\beta} \mathfrak{g}_{\beta\gamma} = \delta^{\alpha}_{\gamma}, \quad (6)$$

and we define \bar{h}^{ab} by

$$\mathfrak{g}^{\alpha\beta} \equiv \sqrt{-\det \eta} (\eta^{\alpha\beta} - \bar{h}^{\alpha\beta}). \quad (7)$$

The vacuum field equations then take the simple form

$$\square \bar{h}^{\alpha\beta} \equiv \eta^{\rho\sigma} \bar{h}^{\alpha\beta}_{,\rho\sigma} = S^{\alpha\beta\kappa\nu}_{\tau\phi\lambda\mu} \bar{h}^{\tau\phi}_{,\kappa} \bar{h}^{\lambda\mu}_{,\nu} + \bar{h}^{\rho\sigma} \bar{h}^{\alpha\beta}_{,\rho\sigma}, \quad (8)$$

where

$$S_{\tau\phi\lambda\mu}^{\alpha\beta\kappa\nu} = - \left[\delta_{\rho}^{(\alpha} \delta_{\sigma}^{\beta)} - \frac{1}{2} \mathfrak{g}^{\alpha\beta} \mathfrak{g}_{\rho\sigma} \right] \left[\delta_{\tau}^{\rho} \delta_{\lambda}^{\sigma} \delta_{\phi}^{\nu} \delta_{\mu}^{\kappa} - 2 \delta_{\tau}^{\rho} \mathfrak{g}^{\sigma\nu} \mathfrak{g}_{\phi\lambda} \delta_{\mu}^{\kappa} + \delta_{\tau}^{\rho} \delta_{\lambda}^{\sigma} \mathfrak{g}_{\phi\mu} \mathfrak{g}^{\kappa\nu} \right. \\ \left. - \frac{1}{2} \mathfrak{g}^{\rho\sigma} \mathfrak{g}_{\tau\lambda} \mathfrak{g}_{\phi\mu} \mathfrak{g}^{\kappa\nu} + \frac{1}{4} \mathfrak{g}^{\rho\kappa} \mathfrak{g}^{\sigma\nu} \left(2 \mathfrak{g}_{\tau\lambda} \mathfrak{g}_{\phi\mu} - \mathfrak{g}_{\tau\phi} \mathfrak{g}_{\lambda\mu} \right) \right]. \quad (9)$$

Equation (8), along with the definition (7), are the equations to be solved for the unknown fields $\bar{h}^{\alpha\beta}$.

Note that so far Eq. (8) is exact; there is no assumption that the $\bar{h}^{\alpha\beta}$ fields are perturbative. If we do treat these fields as perturbative, the post-Minkowski approximation follows by replacing \mathfrak{g} on the right by η to get

$$\square \bar{h}^{\alpha\beta} \equiv \eta^{\rho\sigma} \bar{h}^{\alpha\beta}_{,\rho\sigma} = - \left[\delta_{\rho}^{(\alpha} \delta_{\sigma}^{\beta)} - \frac{1}{2} \eta^{\alpha\beta} \eta_{\rho\sigma} \right] \left[\delta_{\tau}^{\rho} \delta_{\lambda}^{\sigma} \delta_{\phi}^{\nu} \delta_{\mu}^{\kappa} - 2 \delta_{\tau}^{\rho} \eta^{\sigma\nu} \eta_{\phi\lambda} \delta_{\mu}^{\kappa} + \delta_{\tau}^{\rho} \delta_{\lambda}^{\sigma} \eta_{\phi\mu} \eta^{\kappa\nu} \right. \\ \left. - \frac{1}{2} \eta^{\rho\sigma} \eta_{\tau\lambda} \eta_{\phi\mu} \eta^{\kappa\nu} + \frac{1}{4} \eta^{\rho\kappa} \eta^{\sigma\nu} \left(2 \eta_{\tau\lambda} \eta_{\phi\mu} - \eta_{\tau\phi} \eta_{\lambda\mu} \right) \right] \bar{h}^{\tau\phi}_{,\kappa} \bar{h}^{\lambda\mu}_{,\nu} + \bar{h}^{\rho\sigma} \bar{h}^{\alpha\beta}_{,\rho\sigma}. \quad (10)$$

For linearized general relativity, the terms on the right can be ignored and the field equations are simply

$$\square \bar{h}^{\alpha\beta} = 0. \quad (11)$$

These can be solved in closed form as expansions in special functions[24].

In the case of a scalar field model, helical symmetry means that the scalar field Φ is a function only of corotating coordinates $\tilde{x}, \tilde{y}, \tilde{z}$, or $\tilde{r}, \tilde{\phi}, \tilde{z}$, and not of \tilde{t} . The computations for the field then involve only three coordinates. Complications arise when dealing with the components of tensor fields, since computational fields must be “helical scalars,” i.e., functions only of the rotating coordinates. The approach we employ is to define

$$\tilde{\Psi}^{(nn)} = \bar{h}^{tt} \quad (12)$$

$$\tilde{\Psi}^{(n0)} = \sqrt{2} \bar{h}^{tz} \quad (13)$$

$$\tilde{\Psi}^{(n1)} = e^{i\Omega t} (\bar{h}^{tx} - i\bar{h}^{ty}) \equiv U^{(n1)} + iV^{(n1)} = - \left(\tilde{\Psi}^{(n,-1)} \right)^* \quad (14)$$

$$\Psi^{(00)} = \frac{1}{\sqrt{3}} [\bar{h}^{xx} + \bar{h}^{yy} + \bar{h}^{zz}] \quad (15)$$

$$\tilde{\Psi}^{(20)} = \frac{-1}{\sqrt{6}} [\bar{h}^{xx} + \bar{h}^{yy} - 2\bar{h}^{zz}] \quad (16)$$

$$\tilde{\Psi}^{(21)} = e^{i\Omega t} (-\bar{h}^{xz} + i\bar{h}^{yz}) \equiv U^{(21)} + iV^{(21)} = - \left(\tilde{\Psi}^{(2,-1)} \right)^* \quad (17)$$

$$\tilde{\Psi}^{(22)} = e^{2i\Omega t} \left(\frac{1}{2} [\bar{h}^{xx} - \bar{h}^{yy}] - i\bar{h}^{yx} \right) \equiv U^{(22)} + iV^{(22)} = \left(\tilde{\Psi}^{(2,-2)} \right)^*, \quad (18)$$

in which $\tilde{\Psi}^{(nn)}, \tilde{\Psi}^{(n0)}, U^{(n1)}, V^{(n1)}, \tilde{\Psi}^{(00)}, \tilde{\Psi}^{(20)}, U^{(21)}, V^{(21)}, U^{(22)}, V^{(22)}$, are 10 real, helical scalars that carry all the information about the metric.

We denote any of 4 real and 3 complex helical scalars as $\tilde{\Psi}^A$, with A taking the value $nn, n0, n1, \dots$. In terms of these helical scalars the field equations (8) take the form

$$\square \tilde{\Psi}^A - 2i\mu(A)\Omega^2 \partial_{\varphi} \tilde{\Psi}^A + \mu(A)^2 \Omega^2 \tilde{\Psi}^A = \mathcal{Q}^A(\tilde{\Psi}^B), \quad (19)$$

where $\mu(A)$ has the value of 0 for $A = (nn), (n0), (00), (20)$, has the value ± 1 for $A = (n\pm 1), (2\pm 1)$ and has value ± 2 for $A = (2\pm 2)$.

In order to give the details of the source term we must introduce a set of objects $\mathbf{n}, \mathbf{e}_x, \mathbf{e}_y, \mathbf{e}_z$. These objects are described in detail in Ref. [25], and can roughly be considered to be the basis vectors associated with coordinates t, x, y, z . In terms of these, we define the objects

$$\tilde{\mathbf{t}}_{nn} \equiv \mathbf{n}\mathbf{n} \quad (20)$$

$$\tilde{\mathbf{t}}_{n0} \equiv \frac{1}{\sqrt{2}} [\mathbf{n}\mathbf{e}_z + \mathbf{e}_z\mathbf{n}] \quad (21)$$

$$\tilde{\mathbf{t}}_{n,\pm 1} \equiv e^{\mp i\Omega t} \left(\frac{\mp 1}{2} \right) [\mathbf{n}(\mathbf{e}_x \pm i\mathbf{e}_y) + (\mathbf{e}_x \pm i\mathbf{e}_y)\mathbf{n}] \quad (22)$$

$$\tilde{\mathbf{t}}_{0,0} \equiv \frac{1}{\sqrt{3}} [\mathbf{e}_x\mathbf{e}_x + \mathbf{e}_y\mathbf{e}_y + \mathbf{e}_z\mathbf{e}_z] \quad (23)$$

$$\tilde{\mathbf{t}}_{2,0} \equiv \frac{-1}{\sqrt{6}} [\mathbf{e}_x\mathbf{e}_x + \mathbf{e}_y\mathbf{e}_y - 2\mathbf{e}_z\mathbf{e}_z] \quad (24)$$

$$\tilde{\mathbf{t}}_{2,\pm 1} \equiv e^{\mp i\Omega t} \left(\mp \frac{1}{2} \right) [\mathbf{e}_x\mathbf{e}_z + \mathbf{e}_z\mathbf{e}_x] - \frac{1}{2} i [\mathbf{e}_y\mathbf{e}_z + \mathbf{e}_z\mathbf{e}_y] \quad (25)$$

$$\tilde{\mathbf{t}}_{2,\pm 2} \equiv e^{\mp 2i\Omega t} \frac{1}{2} [\mathbf{e}_x\mathbf{e}_x - \mathbf{e}_y\mathbf{e}_y \pm i(\mathbf{e}_y\mathbf{e}_x + \mathbf{e}_x\mathbf{e}_y)], \quad xs \quad (26)$$

which are shown to be helical scalars in Ref. [25]. With this notation the explicit form of the source is [30]

$$\mathcal{Q}^A(\tilde{\Psi}) = \left(\tilde{t}_A^{\alpha\beta} \right)^* S_{\tau\phi\lambda\mu}^{\alpha\beta\kappa\nu} \tilde{t}_B^{\tau\phi} \tilde{t}_C^{\lambda\mu} \left[\tilde{\Psi}_{,\kappa}^B - i\mu(B)\delta_\kappa^t \tilde{\Psi}^B \right] \left[\tilde{\Psi}_{,\nu}^C - i\mu(C)\delta_\nu^t \tilde{\Psi}^C \right] \\ + \tilde{t}_B^{\rho\sigma} \tilde{\Psi}^B \left[\tilde{\Psi}_{,\rho\sigma}^A - i\mu(A)\Omega \left(\delta_\rho^t \tilde{\Psi}_{,\sigma}^A + \delta_\sigma^t \tilde{\Psi}_{,\rho}^A \right) - \mu(A)^2 \Omega^2 \delta_\rho^t \delta_\sigma^t \tilde{\Psi}^A \right]. \quad (27)$$

Here the summation is not only over the tensorial indices, but also over the indices, B, C which range over the 10 values $(nn), (n0), (n \pm 1), (00), (20), (2 \pm 1), (2 \pm 2)$.

Rather than work with the complex fields $\tilde{\Psi}^{(n1)}, \tilde{\Psi}^{(21)}, \tilde{\Psi}^{(22)}$, in practice we work with the real and imaginary parts U^A and V^A , and for $A = (n1), (21), (22)$ Eq. (19) is replaced by

$$\square U^A + 2\mu(A)\Omega^2 \partial_\varphi V^A + \mu(A)^2 \Omega^2 U^A = \text{Real part of } (\mathcal{Q}^A) \quad (28)$$

$$\square V^A - 2\mu(A)\Omega^2 \partial_\varphi U^A + \mu(A)^2 \Omega^2 V^A = \text{Imaginary part of } (\mathcal{Q}^A). \quad (29)$$

The \square operator here, as in Eq. (19), is $\eta^{\alpha\beta} \partial_\alpha \partial_\beta$, and the helically symmetric time derivatives are implemented through the replacement $\partial_t \rightarrow -\Omega(x\partial_y - y\partial_x) = -\Omega\partial_\varphi$, so that

$$\square = \partial_{\tilde{x}}^2 + \partial_{\tilde{y}}^2 + \partial_{\tilde{z}}^2 - \Omega^2 \partial_\varphi^2. \quad (30)$$

The mathematical problem of finding the fields in full general relativity then consists of solving the partial differential equations (19), (28), (29). The post-Minkowskian and linear approximations to general relativity follow from making the appropriate simplifications of \mathcal{Q}^A .

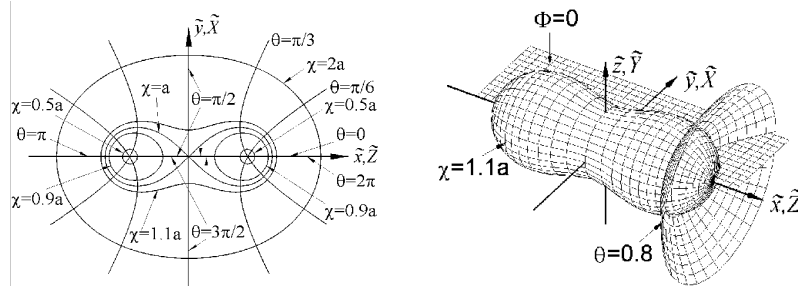


FIG. 1: Two-center bipolar adapted coordinates. On the left is shown curves of coordinates χ and Θ in the $\Phi = 0$ orbital plane. On the right are surfaces of constant χ , Θ , and Φ . At large χ/a the adapted coordinates Θ, Φ are spherical polar angles with respect to the corotating coordinates $\tilde{X}, \tilde{Y}, \tilde{Z}$, a permutation of the coordinates $\tilde{x}, \tilde{y}, \tilde{z}$, discussed in the text.

Computational solutions of the field equations are carried out in an “adapted” corotating coordinate system χ, Θ, Φ illustrated in Fig. 1. These coordinates are two-center bipolar coordinates, defined in terms of the corotating coordinates $\tilde{x}, \tilde{y}, \tilde{z}$. The two “centers” are the coordinate points $\tilde{x} = \pm a, \tilde{y} = \tilde{z} = 0$, points that roughly represent the locations of the black hole sources. At large values of χ/a , the adapted coordinates approach ordinary spherical coordinates with χ the radial coordinate. At small values of χ/a , the adapted coordinates become a reparametrization of spherical coordinates centered on the bipolar points, with the χ coordinate approaching $\sqrt{2a\mathcal{R}}$ where \mathcal{R} is the (corotating) coordinate distance from one of the bipolar centers, and with 2Θ approaching the angle with respect to the \tilde{x} axis. These coordinates are discussed in detail in Ref. [23].

Each of the helical scalar fields is expanded in the form

$$\Psi = \sum_{\ell m} a_{\ell m}^{(A)}(\chi) Y_{\ell m}(\Theta, \Phi). \quad (31)$$

Due to the nature of the coordinates only a few multipoles need to be kept. The argument for this “multipole filtering” is given in Ref. [23], along with numerical results demonstrating its validity.

B. The boundary conditions

The standing wave condition is a procedure rather than a constraint, like Dirichlet, Neuman or Sommerfeld conditions. This procedure is applied in the weak wave zone at some value χ_{\max} of χ that is many times larger than a , and much larger than a wavelength ($1/\Omega$). In this weak wave zone the fields can be treated as perturbations of flat spacetime, and outgoing/ingoing conditions on the perturbations can be imposed. The standing wave procedure for full general relativity starts with the system of equations (4) – (8). An approximate solution for $\bar{h}^{\alpha\beta}$ is put into the right hand side of Eq. (8), both for the explicit appearance of the $\bar{h}^{\alpha\beta}$ terms and through the dependence of the $\mathbf{g}^{\alpha\beta}$ terms on $\bar{h}^{\alpha\beta}$. The right hand side is then treated as known, and Eq. (8) is considered to be a linear equation for $\bar{h}^{\alpha\beta}$. In Ref. [23] it was shown that in adapted coordinates outgoing (+) and ingoing (-) conditions on any of the helical scalars are

$$\frac{1}{\chi} \frac{\partial}{\partial \chi} (\chi \tilde{\Psi}) = \pm \Omega \left(\cos \Phi \frac{\partial \tilde{\Psi}}{\partial \Theta} - \frac{\cos \Theta}{\sin \Theta} \sin \Phi \frac{\partial \tilde{\Psi}}{\partial \Phi} \right). \quad (32)$$

These conditions are used to compute both outgoing and ingoing solutions to the linear equations for each of the helical scalars $\tilde{\Psi}$. The ingoing and outgoing solutions are then averaged, the result is taken as an improved approximation for the field, and the process is iterated.

The convergent result, which we call the standing wave solution, is an exact (numerical) solution of the nonlinear field equations with no net flow of energy inward or outward. The field equations could also be solved for a nonlinear outgoing solution, or a nonlinear ingoing solution. In principle, for nonlinear equations, the standing wave solution is *not* the average of the ingoing and outgoing solutions. In practice, however, it is an excellent approximation for the following reason, which we call “effective linearity.” The ingoing and outgoing solution in the strong field region is negligibly affected by the boundary conditions in the strong field zone, so that the average of the ingoing and outgoing solution there must be the same as the standing wave solution. In the weak wave zone, the solution is completely different for different radiation conditions, but in the weak wave zone the problem is effectively linear, and again the average and the standing wave solutions are very nearly the same.

Effective linearity means that we can treat the standing wave solution as if it were the average, and we can decompose it into approximate ingoing and outgoing solutions. We take the outgoing solution to be our approximation to the solution to the physical problem.

The inner boundary is imposed on quasispherical surfaces, around the bipolar centers, at some small value χ_{\min} of χ . The choice of the numerical value of χ_{\min} is a compromise. The choice of a small value means that the conditions at χ_{\min} will be dominated by the presence of the black hole it surrounds, and the other hole in the binary pair can be considered to have a weak influence. But a small value of χ_{\min} means that the computational regime $\chi_{\min} \leq \chi \leq \chi_{\max}$, includes fields strong enough to cause problems in the convergence of the computational method.

An important point about the inner boundary conditions is made in all previous papers on this method: the details of the inner boundary conditions are equivalent to the details of the sources they represent inside the $\chi = \chi_{\min}$ surface. But the details have almost no effect on the fields in the wave zone, and even in the intermediate $\chi \approx a$ zone. We can, therefore, impose conditions at $\chi = \chi_{\min}$ that represent some reasonable source, and defer the task of adjusting the details. The wave fields, the computed outgoing energy, etc. will be negligibly affected.

Our choice is taken to be the conditions for a single Schwarzschild hole comoving with harmonic coordinates. This reasonable choice was used in our post-Minkowski computations, and hence that choice facilitates comparisons with previous work. The actual form of the boundary conditions have been previously reported [25] and are included here for completeness:

$$\tilde{\Psi}^{\mathbf{nn}} = \left(\frac{4M}{\mathcal{R}} + \frac{7M^2}{\mathcal{R}^2} \right) \gamma^2 - \frac{M^2}{\mathcal{R}^2} \frac{v^2 \gamma^4}{\mathcal{R}^2} \frac{\chi^4}{4a^2} \sin^2(2\Theta) \cos^2 \Phi \quad (33)$$

$$\tilde{\Psi}^{\mathbf{n0}} = \pm \frac{M^2}{\mathcal{R}^2} \frac{v \gamma^2}{\mathcal{R}^2} \frac{\chi^4}{4a^2} \sin^2(2\Theta) \sin \Phi \cos \Phi \quad (34)$$

$$U^{(n1)} = \frac{M^2}{\mathcal{R}^2} \frac{v \gamma^2}{\mathcal{R}^2} \frac{\chi^4}{4a^2} \sin(2\Theta) \cos 2\Theta \cos \Phi \quad (35)$$

$$V^{(n1)} = \left[- \left(\frac{4M}{\mathcal{R}} + \frac{7M^2}{\mathcal{R}^2} \right) v\gamma^2 + \frac{M^2}{\mathcal{R}^2} \frac{v\gamma^4}{\mathcal{R}^2} \frac{\chi^4}{4a^2} \sin^2(2\Theta) \cos^2 \Phi \right] \text{sgn}[\cos \Theta] \quad (36)$$

$$\tilde{\Psi}^{00} = \left(\frac{4M}{\mathcal{R}} + \frac{7M^2}{\mathcal{R}^2} \right) \frac{v^2\gamma^2}{\sqrt{3}} - \frac{M^2}{\sqrt{3}\mathcal{R}^4} \frac{\chi^4}{4a^2} (1 + (\gamma^4 - 1) \sin^2 2\Theta \cos^2 2\Phi) \quad (37)$$

$$\tilde{\Psi}^{20} = - \left(\frac{4M}{\mathcal{R}} + \frac{7M^2}{\mathcal{R}^2} \right) \frac{v^2\gamma^2}{\sqrt{6}} + \frac{M^2}{\sqrt{6}\mathcal{R}^4} \frac{\chi^4}{4a^2} (\cos^2 2\Theta + \gamma^4 \sin^2 2\Theta \cos^2 \Phi - 2 \sin^2 2\Theta \sin^2 \Phi) \quad (38)$$

$$U^{(21)} = \frac{M^2}{\mathcal{R}^4} \frac{\chi^4}{4a^2} \sin 2\Theta \cos 2\Theta \sin \Phi \text{sgn}[\cos \Theta] \quad (39)$$

$$V^{(21)} = - \frac{M^2}{\mathcal{R}^4} \frac{\chi^4\gamma^2}{4a^2} \sin^2 2\Theta \sin \Phi \cos \Phi \quad (40)$$

$$U^{(22)} = - \left(\frac{4M}{\mathcal{R}} + \frac{7M^2}{\mathcal{R}^2} \right) \frac{v^2\gamma^2}{2} - \frac{M^2}{2\mathcal{R}^4} \frac{\chi^4}{4a^2} (\cos^2 2\Theta - \gamma^4 \sin^2 2\Theta \cos^2 \Phi) . \quad (41)$$

$$V^{(22)} = \frac{M^2}{\mathcal{R}^4} \frac{\chi^4\gamma^2}{4a^2} \cos 2\Theta \sin 2\Theta \cos \Phi \text{sgn}[\cos \Theta] . \quad (42)$$

Here, \mathcal{R} , in terms of adapted coordinates, is given by

$$\mathcal{R}^2 \equiv \frac{\chi^4}{4a^2} [1 + \gamma^2 v^2 \sin^2 2\Theta \cos^2 \Phi] , \quad (43)$$

where $v = a\Omega$ is the coordinate speed of the sources and γ is the corresponding Lorentz factor $1/\sqrt{1-v^2}$. The symbol \mathcal{R} is the coordinate distance from a source “point” in a frame comoving with the source; its form in adapted coordinates is derived in Ref.[25]. The \pm in Eq. (34) distinguishes between the condition (+) for the source point at $\Theta = 0$ and the condition (-) for the source point at $\Theta = \pi$.

C. Numerical implementation

In practice one of the issues that requires considerable care in numerically implementing the PSW method is treatment of the boundary conditions. Consider first the outer boundary conditions. For the most part, numerical implementation of boundary conditions (32) consistent with expansion (31) is straightforward. However, special care must be taken with the non-radiative parts of $\tilde{\Psi}^{(nn)}$, $\tilde{\Psi}^{(20)}$, and $\tilde{\Psi}^{(00)}$, as both the analytical and numerical solutions of these fields are dominated by non-radiative modes. In Ref. [24] the general form of the analytical solution for these fields in linearized theory is reported to be

$$\begin{aligned} \Psi^A = & -2K \sum_{\ell=0,2,\dots} \frac{1}{2\ell+1} Y_{\ell 0}^*(\pi/2, 0) Y_{\ell 0}(\theta, 0) \frac{r_{<}^\ell}{r_{>}^\ell} \\ & + 4K\Omega \sum_{\ell=2,4,\dots} \sum_{m=2,4,\dots} m j_\ell(m\Omega r_{<}) Y_{\ell m}^*(\pi/2, 0) Y_{\ell m}(\theta, 0) \text{Im} \left[h_\ell^{(1)}(m\Omega r_{>}) e^{im\varphi} \right] . \end{aligned} \quad (44)$$

Here K is a constant that depends on whether A is (nn) , (20) , or (00) ; $j_\ell(x)$ is the spherical Bessel function of order ℓ ; $h_\ell^{(1)}$ is the spherical Hankel function of order ℓ ; $r_{<} = \min(r, a)$, and $r_{>} = \max(r, a)$.

Expression (44) shows that series solutions for $\tilde{\Psi}^{(n,n)}$, $\tilde{\Psi}^{(2,0)}$, and $\tilde{\Psi}^{(0,0)}$ are dominated by the $\ell = 0$, $m = 0$ mode, which decays as $1/r$ for large r values. Since the radiative part also decays as $1/r$ it is necessary to separate numerically the radiative and non-radiative parts of the solution at large radius. This is accomplished

by setting the following boundary condition for the monopole a_{00} (i.e., the $\ell = 0, m = 0$ mode amplitude) of these fields

$$\frac{\partial}{\partial \chi} a_{00} = -\frac{a_{00}}{\chi}. \quad (45)$$

This is just a mathematical statement that at large distances the dominant part of a_{00} falls off as $1/r$.

The numerical implementation of the inner boundary conditions must also be treated with care. It turns out that some of the conditions in Eqs. (33) – (42) are not to be considered as explicit values to be set at the inner boundary, but rather as regularity conditions on certain of the fields. (It should be understood that not all the fields need to have data imposed to give them a scale. Due to the coupling of fields in the field equations some of the fields are given scale by the coupling to other fields, not by their own boundary data. In practice we do this by replacing Eqs. (35), (39), (40), and (42) with

$$\frac{\partial}{\partial \chi} U^{(n1)} = 0 \quad (46)$$

$$\frac{\partial}{\partial \chi} U^{(21)} = 0 \quad (47)$$

$$\frac{\partial}{\partial \chi} V^{(21)} = 0 \quad (48)$$

$$\frac{\partial}{\partial \chi} V^{(22)} = 0, \quad (49)$$

since this choice has already been used in Ref. [24] and [25].

III. NUMERICAL METHOD

A. Discrete spherical harmonics

Discrete spherical harmonics were introduced first in Ref. [24] as an integral part of the eigenspectral method. In a straightforward approach to their use, spherical harmonics of analytic theory would be evaluated at discrete grid points. We have found that this leads to unacceptable failures of orthogonality, so instead we have used “discrete spherical harmonics” which are orthogonal to the level of machine precision.

To understand these, consider a two dimensional computational grid with $N \equiv n_\Theta \times n_\Phi$ points. The discrete spherical harmonics $Y_{ij}^{(k)}$ are N -dimensional vectors which are conveniently represented by the two indices $1 \leq i \leq n_\Theta$ and $1 \leq j \leq n_\Phi$. Let the matrix $L_{ab,ij}$ be the operator equivalent to the angular Laplace operator evaluated at Θ_a and Φ_b . This operator is therefore defined by

$$[\sin \Theta \nabla_{\text{ang}}^2 f(\Theta, \Phi)]_{ab} \approx \sum_{ij} L_{ab,ij} f_{ij} \quad (50)$$

where $f(\Theta, \Phi)$ is an arbitrary function and where $f_{ij} = f(\Theta_i, \Phi_j)$. The approximation symbol in the relationship is due to the truncation error induced by the finite difference representation of the derivatives on the left.

The discrete spherical harmonics $Y_{ij}^{(k)}$ are defined to be the solutions of the generalized eigenvector problem

$$\sum_{ij} L_{ab,ij} Y_{ij}^{(k)} = -\Lambda \sin \Theta_a Y_{ab}^{(k)}, \quad (51)$$

together with the normalization condition

$$\sum_i \sum_j Y_{ij}^{(k)} Y_{ij}^{(k')} \Delta \Theta \Delta \Phi = \delta_{kk'}. \quad (52)$$

Details of the construction of the matrix operator $L_{ab,ij}$ and of the computation and properties of the eigenvectors can be found in Refs/ [24] and [30].

B. The use of symbolic manipulation

It is clear that most of the aspects involved in the computation of fully relativistic fields with the eigenspectral method (i.e., with adapted coordinates, multipole filtering, and discrete spherical harmonics) are not conceptually difficult, but are technically difficult to implement. The advantages of the eigenspectral method, explained in detail in references [24, 25], are offset by an increased complexity in the form of the equations. The several stages required by a typical algorithmic solution to a problem within the eigenspectral method are illustrated in Fig. 2(a). During the early development of the PSW program most of the work at these stages was carried out by a human being, with the computer used only for the final numerical solution of the equations.

The fact that most of the stages depicted in Fig. 2(a) are algorithmic in nature suggested the idea of developing a computational framework to deal with the different aspects of the computation. The framework was designed to ease the numerical implementation of any level of approximation within the PSW model (i.e., linear, PM or fully relativistic) by reflecting the workflow of Fig. 2(a). This framework included the implementation of several sets of tools for the PSW project within *Maple*TM, a general-purpose computer algebra system (CAS) software package.

Three different set of tools were developed for the PSW project. The first set corresponds to the conversion of an equation in Minkowski coordinates $t, \tilde{x}, \tilde{y}, \tilde{z}$ into adapted coordinates. The role of a second set of tools was to perform the conversion to finite difference form of any given differential equation. Finally a third set corresponds to tools implemented to convert *Maple* expressions into C functions. This final set includes tools that are able to create all the different C functions related to the projections over spherical harmonics and the construction of the matrix system that has to be solved at each iteration either in a perturbative or exact scheme as described in Ref. [25]. The code generated by these tools was later embedded into a bigger infrastructure developed in C. The C infrastructure essentially takes care of runtime issues, such as the allocation of memory and the interface of advanced numerical routines in LAPACK for matrix inversion and eigenvector computation for the routines generated by *Maple*.

The implementation process for a given model within the PSW-eigenspectral method (namely, linear gravity, post-Minkowski, or full general relativity) is streamlined through these tools. First the differential equations have to be provided in completely explicit form. The first set of tools is then applied to these equations, rendering the equations in adapted coordinates. The equations that are output are next passed through the second set of tools, to put them into finite difference form. Finally, the output of this process is passed through the third set of tools in order to obtain the C code.

The net effect of the use of these tools “raises the bar” for the implementation of numerical models with the eigenspectral method, in that most of the process is performed by the computer, as Fig. 2(b) illustrates. We emphasize that the use of symbolic manipulation was indispensable to the last phase of the PSW-eigenspectral program. This leads us to suggest that a similar eclectic use of algebraic manipulation software and numerical programming is a powerful approach not only for our problem but for other problems in which code must be generated for complex and lengthy mathematical expressions for which human coding is prone to error. However it is worth noting that neither *Maple* nor any other computer algebra system is able by itself can directly generate the C expressions required for this kind of project. Although most algebra systems features parsers to generate C code most of the time the native parsing algorithm can not deal with some subtleties. Some of these subtleties include type specification for intermediate variables, data type signature of functions, the appropriate translation of some mathematical functions and the creation of header files among others. For the present work it became necessary to modify the native parser of *Maple* in order to deal with these subtleties. In particular the syntax definition of the C parser was enlarged in order to include some mathematical functions while the parsing algorithm was modified in order to ensure the correct signature for the functions defined during the automated process. In addition some fine tuning was performed in the parser algorithm in order to avoid incorrect or unnecessary operations in the translated code, such as some type casts or incorrect array indexing. These kind of subtleties must be addressed and tailored to the occasion by any other project that wants to use a similar approach of the mixing Computer Algebra Systems and analytic tools.

IV. NUMERICAL RESULTS

The ultimate unknowns for which we actually solve are the coefficients $a_{\ell m}^A(\chi)$ of the expansion of the fields $\tilde{\Psi}^A$ in Eq. (31). The equations for these unknown $a_{\ell m}^A(\chi)$ are the field equations (19), along with the appropriate inner and outer boundary conditions. In the source term Q^A for the field equations, the

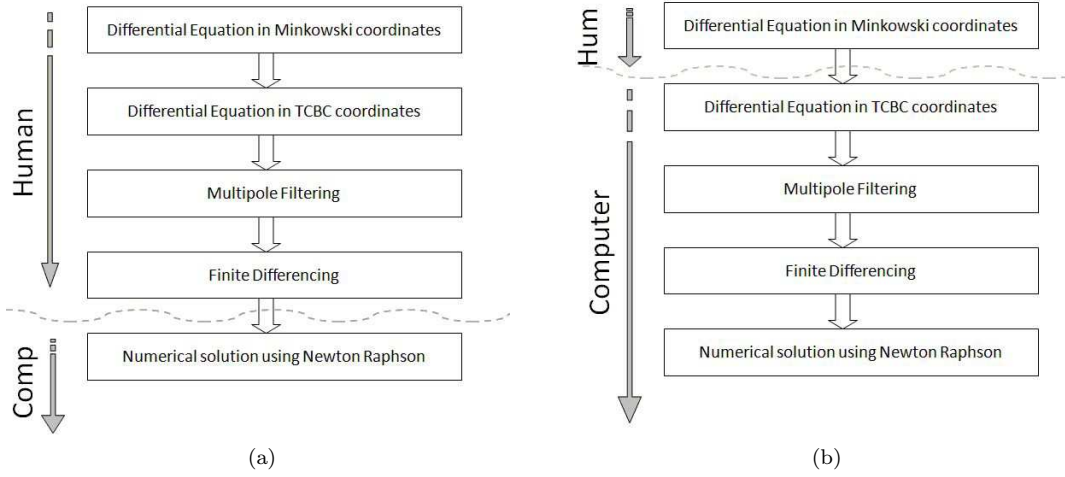


FIG. 2: The process of implementing numerical modeling has been modified by the use of *Maple*. The aid of a computer algebra system has allowed the computer to handle a great deal of the “analytic” work, significantly simplifying the role of the programmer in the development of numerical code

dependence on $a_{\ell m}^A(\chi)$ occurs both in the explicit quadratic appearance of $\tilde{\Psi}^A$ on the right in Eq. (27), and through the very complicated dependence of $S_{\tau\phi\lambda\mu}^{\alpha\beta\kappa\nu}$ on $\tilde{\Psi}^A$ encoded in the equations (6), (7) and (12)–(18). In our work on the post-Minkowski approximation[25] only the first dependence was kept, since inclusion of the dependence through $S_{\tau\phi\lambda\mu}^{\alpha\beta\kappa\nu}$ would have gone beyond the order of the approximation. But in the present work, for the full equations of general relativity, we cannot ignore this deeper nonlinearity. In fact, it is precisely this dependence that, in our formalism, distinguishes full general relativity from the second-order post-Minkowski approximation. The complexity of this nonlinearity, however, leads to a practical problem.

In our work, here and previously, with nonlinear equations, the mathematical problem to be solved was cast into the form $L(y) = F(y)$ in which L is a linear operator on the unknown function, or set of functions y . A solution could be sought in two ways. A direct iteration could be used in which an approximate solution y_n is substituted into $F(y)$ and the linear equation $L(y_{n+1}) = F(y_n)$ for a new approximation y_{n+1} is solved, with appropriate boundary conditions. Alternatively, Newton-Raphson iteration can be used. In this method a linear equation is found by expanding the y dependence of $F(y)$ about $F(y_n)$, with a Jacobian playing the role of the derivative of F with respect to the fields y . Newton-Raphson iteration is expected to have better convergence properties than direct iteration, and this was indeed found to be the case in previous work.

In principle, then, it is a Newton-Raphson scheme that is to be sought. But due to the complicated dependence of $S_{\tau\phi\lambda\mu}^{\alpha\beta\kappa\nu}$ on $a_{\ell m}^A(\chi)$ this does not turn out to be feasible. With *Maple* generated code the evaluation of the Jacobian needed in the Newton-Raphson method becomes unreasonable long. The main reason for this is that the code generated by *Maple* is optimized for execution time by unrolling lengthy evaluations explicitly in several steps using several temporary variables. As a consequence this highly optimized code is extremely lengthy in terms of code lines. As the number of terms given to *Maple* increases so does the code that must be compiled. If the number of terms is high enough the raw code generated with the *Maple* tools becomes so lengthy that it is impossible to compile. This has severely limited the applicability of this automated process for Newton-Raphson methods for a fully relativistic model. For this reason the fully relativistic model was ultimately implemented using a direct iteration scheme.

We have found that the use of direct iteration does not seem to be a major problem. In particular, models with parameters that allowed convergence for post-Minkowski models with Newton-Raphson iteration have been found to converge in full general relativity with direct iteration. One reason for this, is that we have limited our application of the full general relativity models to those for which the post-Minkowski approximation is valid. As explained in Ref. [25], this means that χ_{\min} must not be chosen very small, to avoid very strong nonlinearities. This in turn leads to the constraint on model parameters[25]

$$2\sqrt{2}a\Omega \ll \chi_{\min}/a \ll \sqrt{2}. \quad (53)$$

With this restriction on field strengths convergence has been found to be very good.

This successful convergence is illustrated in Fig. 3 for $\tilde{\Psi}^{(2,0)}$. These results show that convergence is attained after 3 to 4 iterations for angular velocity $\Omega = 0.15$; similar or faster convergence is found for all smaller values

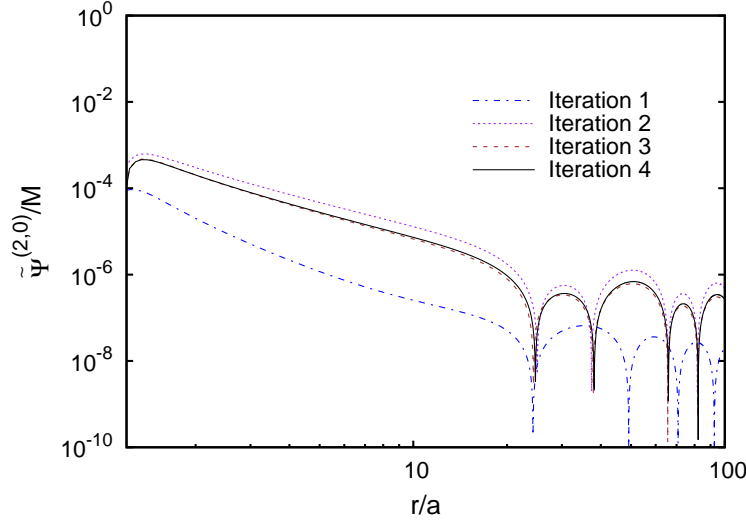


FIG. 3: Typical convergence of fully relativistic $\tilde{\Psi}^{(2,0)}$ using direct iteration. The field is shown as a function of coordinate radius along a line in the orbital plane approximately through the source points (i.e., at $\Theta = \Delta\Theta$). The simulation parameters here are $\Omega = 0.15$, $n_\chi \times n_\Theta \times n_\phi = 1750 \times 16 \times 32$, with $\chi_{\min}/a = 0.50$. The computation includes all multipoles up to $\ell = 3$ (monopole and quadrupole terms kept) although the monopole term a_{00} is not included in the results displayed.

of Ω . We usually consider $\Omega = 0.15$ to be the limit of the angular velocity for which the PSW method gives a good approximation to the outgoing solution.

A very important consideration for the success of the computations, and of the PSW approach, is the value of χ_{\min} , since this parameter determines the maximum field strength encountered in the computation. Moreover, results that are sensitive to the choice of χ_{\min} raise questions about the underlying assumption in the PSW approach that the details of the inner boundary condition are not important to the fields except very near the inner boundary. Figures 4 show the results for all fields, for a model with $\Omega = 0.15$.

These results, show somewhat mixed results for the insensitivity to the value of χ_{\min} . For the “coulombic” field $\tilde{\Psi}^{(n,n)}$ the computed result is particularly insensitive to χ_{\min} . Several of the fields show significant differences in the results for the three values of χ_{\min} . One would expect that the results for the largest value of χ_{\min} should have errors in representing the boundary conditions appropriate for a “point” particle, since $\chi_{\min}/a = 0.6$ is not really justified as a “near source” surface. One might expect better agreement between the two smaller values of χ_{\min} , since both inner boundaries are reasonably close to the source “points.” The results tend to confirm this, though with exceptions. Of particular interest are the results for $U^{(2,2)}, V^{(2,2)}$, since these fields carry the information about gravitational waves in the weak wave zone. For these fields the results for $\chi_{\min}/a = 0.45$ and $\chi_{\min}/a = 0.3$ agree moderately well in phase, but have amplitude differences as large as a factor of 2. A study of the origin of this difference will help clarify the nature of the correct boundary conditions. It should be noted that the computations of the fields within full general relativity have turned out to be less sensitive to the choice of χ_{\min}/a than are the post-Minkowski computations. In some way, the inclusion of the dependence of $S_{\tau\phi\lambda\mu}^{\alpha\beta\kappa\nu}$ on the fields moderates the sensitivity of the results to χ_{\min}/a .

Another type of comparison is presented in Figs. 5, the comparison of computations based on linearized, post-Minkowski and fully relativistic models for $\Omega = 0.075$ and $\chi_{\min}/a = 0.4$. The monopole term a_{00} is not included in the results shown for $\tilde{\Psi}^{(0,0)}$, $\tilde{\Psi}^{(2,0)}$, and $\tilde{\Psi}^{(n,n)}$. The results show that $\tilde{\Psi}^{(n,n)}$ and $\tilde{\Psi}^{(n,1)}$ are very well approximated within the post-Minkowski model. All other fields differ in more or less a significant way with respect to the post-Minkowski results, showing that the fully relativistic contributions are of significance, even for the moderate field strengths of these computations. In this connection it should be noted that the field $\tilde{\Psi}^{(n,n)}$ is very well approximated by lower order approximations. It is only this field that was used in the source term for the iterations in Ref. [25]. Thus, it is not the imperfections in $\tilde{\Psi}^{(n,n)}$ that are the basis of the inaccuracies, but rather the suppressed dependences on additional fields.

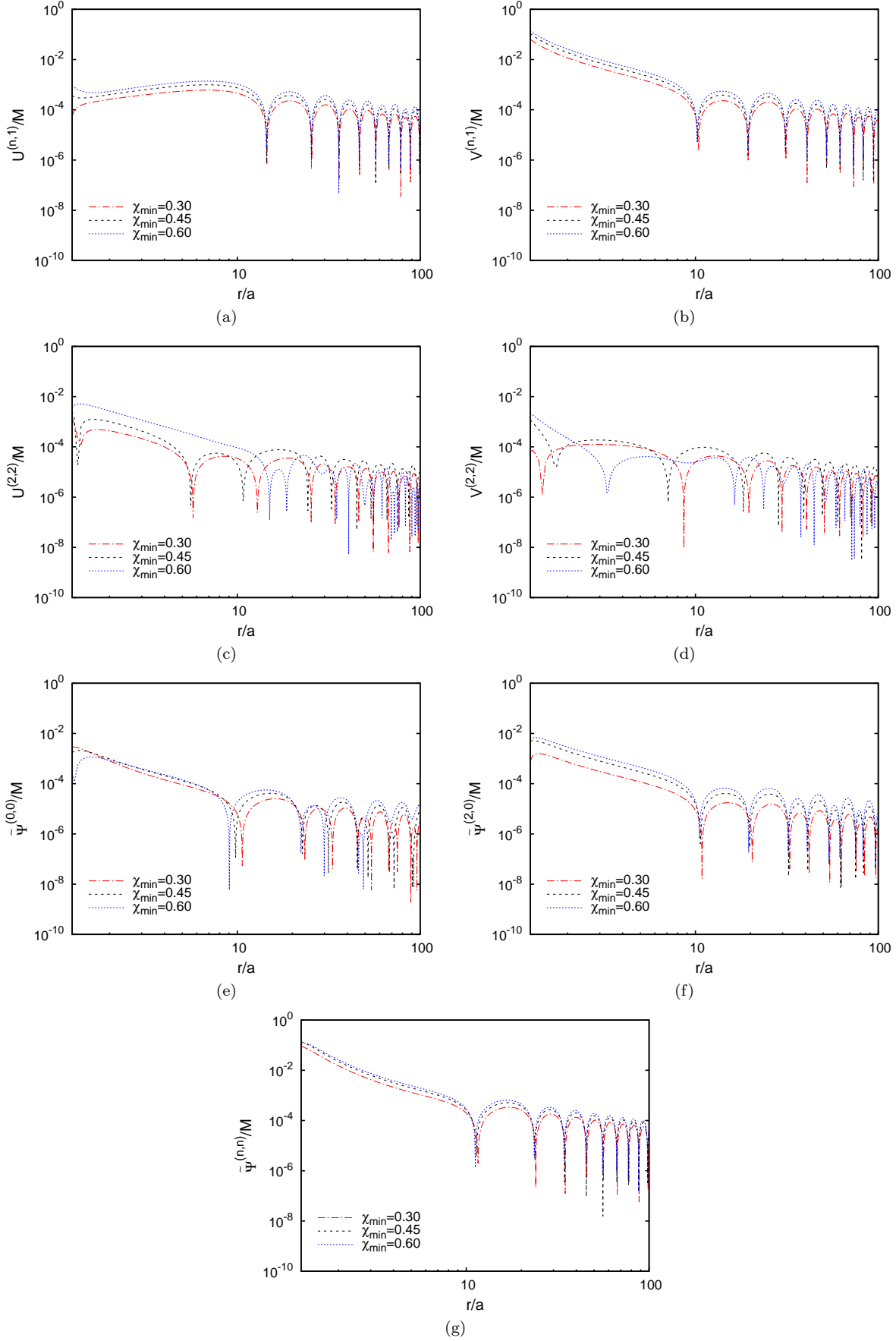


FIG. 4: Comparison of results for direct iteration of relativistic computations as function of χ_{\min} for $\Omega = 0.15$. Fields are shown in the orbital plane along a line approximately through the source points. These results reveal that the location of the inner boundary is less important in fully relativistic models than in post-Minkowski models described in [25], specially for $\tilde{\Psi}^{(n,n)}$.

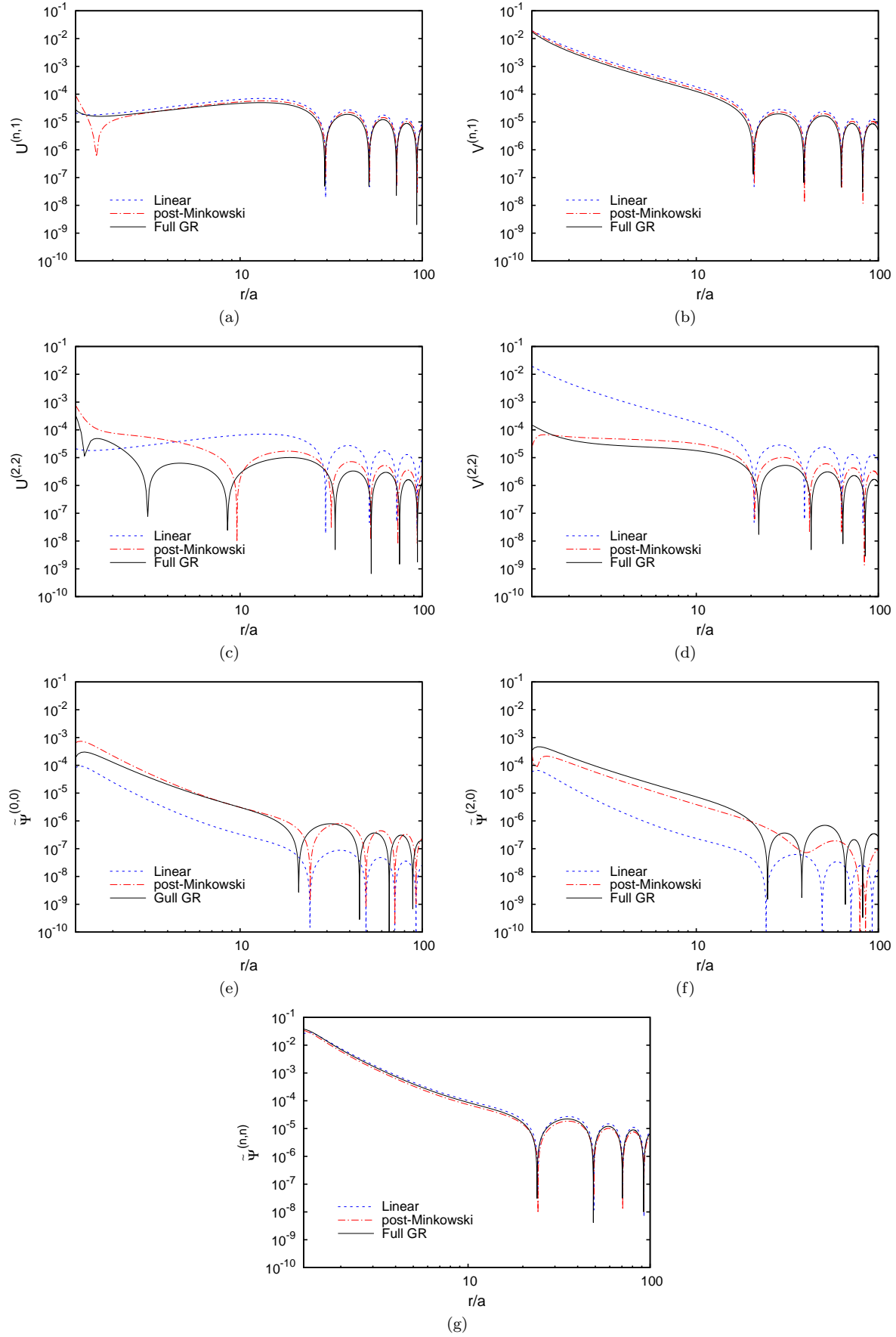


FIG. 5: Comparison between linearized, post-Minkowski and fully relativistic computations with $\Omega = 0.075$. The computations used a numerical grid of $n_\chi \times n_\Theta \times n_\Phi = 1750 \times 16 \times 32$, with $\chi_{\min} = 0.40a$ and $\chi_{\max} = 100a$.

V. DISCUSSION AND CONCLUSIONS

The results presented in the previous section for the fully relativistic case show the same convergence rate as was found for the directly iterated post-Minkowski approximation and show similar limitations in field strength as the Newton-Raphson method for the post-Minkowski approximation. The results also reveal that the nonlinearities present in the fully relativistic model produce important changes in the numerical solutions for most of the fields. For the most important field of the post-Minkowski approximation $\tilde{\Psi}^{(n,n)}$, it is comforting to note that there is excellent agreement of the post-Minkowski and fully relativistic results. The fact that $\Psi^{(n,1)}$ is also well represented by the post-Minkowski computation is also a good sign. These good agreements are expected qualitatively since the post-Minkowski approximation is correct up to second order in the small parameter M/\mathcal{R} while $\Psi^{(n,n)}$ and $\Psi^{(n,1)}$ are of order 1 and 1.5, respectively, in the same parameter. In this sense the relativistic results confirms the validity of the post-Minkowski approximation.

It is important to mention not only the strengths of the method but also its shortcomings. First, the use of adapted coordinates gives a solution on an irregular computational grid on the Minkowski background of the problem. As a consequence the results obtained from the computations require a difficult interpolation if they are to be compared with other results or used as initial data for evolution codes. Second, the method is inherently limited in its accuracy. Higher accuracy, would ultimately require more multipoles, and an increase in the number of multipoles adds to the size of the equation set to be generated by *Maple*, and to the compilation problem.

The current accuracy, however, is sufficient for us to see in the results presented in the previous section that there is sensitivity of the computed fields to the location of the inner boundary χ_{\max} . The inner boundary conditions used for the computations are those for a spherically symmetric mass point, or Schwarzschild hole, boosted so that it is instantaneously comoving with the rotating coordinates. (For a detailed discussion see Ref. [25]). This is, of course, an approximation that ignores the tidal effects of the two source points on each other and the fact that the sources are not moving in straight lines of a Minkowski background. That approximation would be adequate at sufficiently small Ω , but – the results suggest – not at $\Omega = 0.15/a$.

Improved inner boundary conditions are an important application of the PSW method, since this is part of the use of the method to study radiation reaction. But the issue of the inner boundary condition may not be separable from the issue of the gauge condition, which might explain the sensitivity of the results to χ_{\max} even for the relatively small angular rotation rate $\Omega = 0.15/a$. The “gauge issue” is the fact that we have used a specific gauge, that of Eq. (5), but we have not enforced or checked that gauge in the solution. If the problem is well posed then there should be a solution which can be transformed to this gauge. The question of well-posedness directs attention to the inner boundary condition, and the multipoles at the inner boundary. The coarsest parameter in those boundary conditions is simply the mass that we ascribe to the source, a mass that we have linked to the angular velocity Ω through the nonrelativistic Kepler law. One would certainly expect relativistic corrections to that relationship, so in a sense our solution of the fully general relativistic problem has omitted an important source of nonlinearity.

With the adapted coordinate method we have demonstrated that the PSW computations can be brought to a level of accuracy adequate for studying features of the strong fields and inner boundary conditions. It is therefore capable, in principle, of giving useful insights about radiation reaction contained in the details of the near fields. The method can also be used in the future to provide a quasistationary sequence of simulation parameters (i.e., mass, orbital radius and angular velocity). Such sequence will represent more than adequately the slow inspiral process of the binary. The main challenge for this approach is that it is important to show that we are comparing the “same” system at different radii (i.e., that some physical quantities are conserved although energy is lost during the process). For binary neutron stars the baryon number must be unchanged. In the case of black holes the issue is more difficult, since the total mass of the system decreases as energy is emitted. However the local mass of the black holes should not change; this local mass could be calculated at each stage of the sequence using numerical codes designed to detect horizons locally, as described by Ashtekar *et al* [35].

The current work has solved the problem with the accuracy that was sought, and a broader lesson might lie in that success. The success was achieved through the combination of a Computer Algebra System such as *Maple* and numerical programming. This combination can be a powerful approach to some problems that requires not only fast and sophisticated numerical algorithms but also a fast and sophisticated implementation process. The lesson in the PSW program is that the use of a highly analytical approach to the problem (adapted coordinates and multipole filtering) translated into an increased complexity in the algebraic form of the equation. While humans are prone to errors when manipulating lengthy expressions, computers are not. Leaving the details of the manipulation and coding to an algebraic manipulation language is a natural choice for this sort of problems. Of course such an approach involves the development of tools adapted to the needs

of a particular project within *Maple* or any similar development platform, which can be quite challenging. However, once the tools are developed and benchmarked the correctness of the numerical implementation is guaranteed, which is a highly desirable feature for projects involving complex numerical implementations.

VI. ACKNOWLEDGMENT

We gratefully acknowledge the support of NSF grants PHY 0554367, and NASA grant ATP03-0001-0027. We thank Benjamin Bromley, Christopher Beetle, John Friedman and Stephen Lau for many useful discussions and suggestions.

-
- [1] F. Pretorius, Phys. Rev. Lett. **95**, 121101 (2005).
 - [2] F. Pretorius, Class. Quant. Grav. **23**, S529 (2006).
 - [3] F. Pretorius and D. Khurana, Class. Quant. Grav. **24**, S83 (2007).
 - [4] U. Sperhake, V. Cardoso, F. Pretorius, E. Berti, J. A. Gonzalez, Phys. Rev. Lett. **101**, 161101 (2008).
 - [5] M. Campanelli, C. O. Lousto, P. Marronetti, and Y. Zlochower, Phys. Rev. Lett. **95**, 111101 (2006).
 - [6] M. Campanelli, C. O. Lousto, and Y. Zlochower, Phys. Rev. D **73** 061501(R) (2006).
 - [7] M. Campanelli, C. O. Lousto, Y. Zlochower, and D. Merritt, Phys. Rev. Lett. **98**, 231102 (2007).
 - [8] J. G. Baker, J. Centrella, D.-I. Choi, M. Koppitz, and J. van Meter, Phys. Rev. Lett. **96**, 111102 (2006).
 - [9] J. G. Baker, J. Centrella, D.-I. Choi, M. Koppitz, and J. van Meter, Phys. Rev. D **73**, 104002 (2006).
 - [10] J. G. Baker, J. Centrella, D.-I. Choi, M. Koppitz, J. van Meter, and M. Coleman Miller, Astrophys. J. **653**, L93 (2006).
 - [11] J. G. Baker, M. Campanelli, F. Pretorius, and Y. Zlochower, Class. Quant. Grav. **24**, S25, (2007).
 - [12] J. G. Baker, W. D. Boggs, J. Centrella, B. J. Kelley, S. T. McWilliams, M. Coleman Miller, James R. van Meter, Astrophys. J. **682**, 29 (2008).
 - [13] J. G. Baker, W. D. Boggs, J. Centrella, B. J. Kelley, S. T. McWilliams, and James R. van Meter, Phys. Rev. D **78**, 044046 (2008).
 - [14] P. Diener, F. Herrmann, D. Pollney, E. Schnetter, E. Seidel, R. Takahashi, J. Thornburg, and J. Ventrella, Phys. Rev. Lett. **96**, 121101 (2006).
 - [15] J. A. Gonzalez, U. Sperhake, B. Bruegmann, M. Hannam, and S. Husa, Phys. Rev. Lett. **98**, 091101 (2007).
 - [16] M. Koppitz, D. Pollney, C. Reisswig, L. Rezzolla, J. Thornburg, P. Diener, and E. Schnetter, Phys. Rev. Lett. **99**, 041102 (2007).
 - [17] L. Rezzolla, P. Diener, E. N. Dorband, D. Pollney, C. Reisswig, E. Schnetter, and J. Seiler, Astrophys. J. **674**, L29 (2008).
 - [18] U. Sperhake, E. Berti, V. Cardoso, J. A. Gonzalez, B. Bruegmann, M. Ansorg, Phys. Rev. D **78**, 064069 (2008).
 - [19] J. T. Whelan, W. Krivan, and R. H. Price, Class. Quant. Grav. **17**, 4895 (2000).
 - [20] J. T. Whelan, C. Beetle, W. Landry, and R. H. Price, Class. Quant. Grav. **19**, 1285 (2002).
 - [21] R. H. Price, Class. Quant. Grav. **21**, S281 (2004).
 - [22] Z. Andrade *et al.*, Phys. Rev. D **70**, 064001 (2004).
 - [23] B. Bromley, R. Owen and R. H. Price Phys. Rev. D **71**, 104017 (2005).
 - [24] C. Beetle, B. Bromley, and R. H. Price, *Phys Rev D* **74**, 024013 (2006).
 - [25] C. Beetle, B. Bromley, N. Hernández and R. H. Price, *Phys. Rev. D* **76**, 084016 (2007), preprint gr-qc/0708.1141.
 - [26] L. D. Landau and E. M. Lifschitz, *The Classical Theory of Fields*, translated by M. Hamermesh, (Addison-Wesley, Reading Mass., 1962), Sec. 100.
 - [27] C. W. Misner, K. S. Thorne and J. A. Wheeler, *Gravitation* (Freeman, San Francisco, 1973), Sec. 20.3.
 - [28] C. R. Johnson, Phys. Rev. D **4**, 295 (1971); Phys. Rev. D **4**, 318 (1971); Phys. Rev. D **4**, 3555 (1971); Phys. Rev. D **5**, 1916 (1972).
 - [29] J. Van Meter, unpublished PhD thesis, University of California, Davis, 1999.
 - [30] Napoleón Hernández, unpublished PhD thesis, University of Utah, Salt Lake City, 2007.
 - [31] S. Weinberg, *Gravitation and Cosmology: Principles and Applications of the General Theory of Relativity*, (John Wiley and Sons, New York, 1972), p. 181.
 - [32] The coordinates X, Y, Z here have no relations to the Minkowski coordinates X, Y, Z used in Refs. [22, 23, 24].
 - [33] C. W. Misner, K. S. Thorne and J. A. Wheeler, *Gravitation* (Freeman, San Francisco, 1973), Sec. 18.1.
 - [34] S. R. Lau and R. H. Price *Journal of Comp. Phys.* **227**, 1126 (2007), preprint gr-qc/0702050.
 - [35] A. Ashtekar, C. Beetle et al. *Phys. Rev. Lett.* **85**, 3564 (2000)